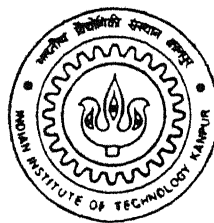


FORCE MONITORING IN DRILLING CONSIDERING IN-PROCESS VIBRATION

by

K. JANARDHANA REDDY



711
11/11/10
12/06/11

DEPARTMENT OF MECHANICAL ENGINEERING
INDIAN INSTITUTE OF TECHNOLOGY KANPUR

June, 1999

FORCE MONITORING IN DRILLING CONSIDERING IN-PROCESS VIBRATION

A Thesis Submitted

in Partial Fulfilment of the Requirements

for the Degree of

MASTER OF TECHNOLOGY

by

K.JANARDHANA REDDY



to the

DEPARTMENT OF MECHANICAL ENGINEERING

INDIAN INSTITUTE OF TECHNOLOGY KANPUR

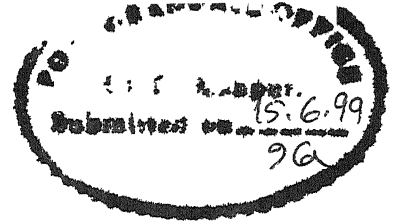
JUNE, 1999

20 OCT 1999 | ME
CENTRAL LIBRARY
I.I.T., KANPUR

No. A 129554

7-11
101-1000
DS-100

CERTIFICATE



It is certified that the work contained in the thesis entitled " FORCE MONITORING IN DRILLING CONSIDERING IN-PROCESS VIBRATION ", by K. JANARDHANA REDDY has been carried out under my supervision and that this work has not been submitted elsewhere for a degree.

 15.6.99
Dr. S.K. CHOUDHURY

Associate Professor

Dept. of Mechanical Engineering

I.I.T. Kanpur

June, 1999

ACKNOWLEDGEMENTS

I would like to express my deep felt gratitude and appreciation to my thesis supervisor Dr. S.K.Choudhury for his skillful guidance, constant supervision, timely suggestions, constructive criticisms in completing of this project within the stipulated time.

I am thankful to Mr. R.M.Jha, Mr. V.Raghuram, Mr. H.P.Sarma, Mr. Namdeo and Mr. Anil for their help during experimentation. Their experience and expertise has been of great help in solving the practical problems encountered.

Many special thanks to all students of the manufacturing science stream for maintaining lively atmosphere with discussions. My special thanks to Sridhar, Paturi, P.S.S.Raju and Venugopal for their help in the preparation of final experimental setup and in writing the thesis report.

I would also like to thank Crao, Sarath, Vinod, Raju, Venumadhav, *Chandu*², Giraka, Gopal, and many other friends for their constant inspiration and suggestions during my course of study at IIT, KANPUR.

I have no words to express my thanks to my parents and my family members who have been constant source of inspiration to me. I wish to thank all my friends and well wishers who made my stay at IIT, KANPUR, memorable and pleasant.

K.Janardhana Reddy

Contents

List of Figures	iii
List of Tables	v
Nomenclature	vi
Abstract	viii
1 Introduction	1
1.1 General Introduction	1
1.2 Vibration in metal cutting	2
1.3 Literature Review	3
1.4 Organization of Thesis	8
2 Theoretical Analysis	10
2.1 Characteristics of Vibration in Drilling	10
2.2 Torque and Thrust force in Drilling	14
3 Experimental Procedure and Set-up	18
3.1 Vibration measuring system	18
3.1.1 Accelerometer:	18
3.1.2 Pre-amplifier:	19
3.1.3 Microphone Amplifier:	20

3.1.4	Displacement Measurement	20
3.2	Measurement of forces in Drilling	21
3.2.1	Principle of dynamometer	22
3.2.2	Working of dynamometer in the present case	22
3.3	Multiple Regression Analysis	25
3.3.1	Design for fitting second order model	26
3.3.2	Least square estimation of the regression coefficients	26
3.4	Planning of experiments	28
3.5	Experimental Procedure	29
4	Results and Discussions	31
4.1	Validation of Regression Model	32
4.2	Feasibility Study	34
4.3	Effect of various parameters	35
5	Conclusions and Scope of future work	42
5.1	Conclusions	42
5.2	Scope of the future work	43
A	Forces in Drilling	47
B	Specifications	49

List of Figures

1.1	An idealized contour of primary deformation zone [11]	7
2.1	Change in Cutting force for an Undeformed chip thickness decreasing due to vibration [16]	11
2.2	Change in Cutting force for an Undeformed chip thickness increasing due to vibration [16]	13
2.3	Relationship between Thrust force (F_Q) and the undeformed thickness t as the tool vibrates in the path indicated by arrows	13
2.4	Development of Torque and Thrust during drilling	15
3.1	Schematic drawing of a piezoelectric accelerometer	19
3.2	Set-up for vibration measurement on the workpiece	20
3.3	Spoked-wheel dynamometer for the measurement of drilling thrust(F) and torque(M).	23
3.4	Deflection scheme of spoked-wheel	24
3.5	Wheatstone bridge for measurement of (a) Thrust force (b) Torque. . .	24
3.6	Treatment combinations in a 3^3 design	29
3.7	Schematic diagram of experimental set-up	30
4.1	Comparison of Experimental and Empirical Thrust force values	32
4.2	Comparison of Experimental and Empirical Torque values	34
4.3	Comparison between Experimental and Empirical Thrust force values for additional verification tests.	35

4.4	Comparison between Experimental and Empirical torque values for additional verification tests	36
4.5	Cutting speed vs Thrust force	37
4.6	Cutting speed vs Torque	38
4.7	Amplitude of vibration vs Thrust force	39
4.8	Amplitude of vibration vs Torque	39
4.9	Feed vs Thrust force	40
4.10	Feed vs Torque	40
4.11	Diameter of Drill vs Thrust force	41
4.12	Diameter of Drill vs Torque	41

List of Tables

4.1	Experimental Data	33
4.2	Cutting conditions and Experimental results for additional verification tests	36

Nomenclature

b	Width of cut
c	Chisel edge length
d	Drill diameter
f	Feed
l	Length of the flank face/workpiece contact area
m	Ratio (c/d)
p	Semi point angle
t	Undeformed thickness
F'_P	Cutting force when undeformed chip thickness decreasing
F'_Q	Thrust force (Vertical) when undeformed chip thickness decreasing
F''_P	Cutting force when undeformed chip thickness increasing
F''_Q	Thrust force when undeformed chip thickness increasing
F, M	Thrust force and Torque respectively
F_T	Force acting on drill directed to axis
F_C	Force acting on drill perpendicular to drill axis
F_{ch}	Force from the chisel edge
$F_{friction}$	Frictional force
M_{ch}	Moment from the chisel edge
$M_{friction}$	Moment due to friction
F_o, M_o	Thrust force and torque at the lips

F', M'	Thrust force and torque at the chisel edge
F'', M''	Thrust force and torque generated at the margins
L	Length of primary deformation zone ahead of the cutting edge
R	Resultant force
R'	New resultant force
N	Cutting speed
N_e	Effective cutting speed
S	Shear strength of the workpiece material in the "as-received" condition, i.e., before it undergoes work hardening resulting from the strains by the cutting process
P_1	Mean normal stress acting ahead of the cutting edge
P_m	Pressure acting over the flank/workpiece contact area
α	Rake angle
α_e	Effective rake angle
β	Friction angle
β'	New friction angle
ϕ	Shear angle
ϕ_e	Effective shear angle
$\Delta\phi$	Change in shear angle
ϕ_n	Merchant normal shear plane angle
δ	Change in rake angle due to change in undeformed thickness
τ	Shear stress
μ	Coefficient of friction between workpiece and tool material in the flank face contact area

k_1, k_2, E, G, B, H Constant coefficients

J, Q, U, V

Subscripts

c Parameter at the chisel edge

ABSTRACT

A knowledge of the cutting forces is required to assist engineers to design machine tools, jigs and fixtures, as well as to select economic cutting conditions. The forces of interest in drilling operations are the thrust force along the axis of rotation and the torque. Under dynamic conditions amplitude of relative vibration between the tool and the workpiece effects the forces on the tool. Through the use of real-time thrust/torque monitoring system, one may use the torque/thrust models as tool failure criterion.

In this study, thrust force and torque monitoring in drilling has been developed. This approach has used the relationship between the force signals and amplitude of relative vibration between the tool and the workpiece as well as the cutting parameters. Research work has shown that any change in the cutting condition of the tool, such as caused by increased amount of amplitude of vibration, would also appear as changes in the signature profile of the cutting force spectrum. So strong correlation exists between the force characteristic and the amplitude of vibration progress. Experiments were conducted to study the effect of the cutting parameters and the amplitude of relative vibration on the force signals and to develop a second order regression model for force signals. The measured force signals, amplitude of vibration and the cutting parameters obtained by drilling C-45 steel with HSS drill bits.

Additional tests have been conducted to verify the feasibility of the model proposed. Results showed that the proposed models can be generalized to estimate the thrust force and the torque for any set of cutting conditions, hence force monitoring can be achieved for the cases where the use of dynamometer is not possible.

Chapter 1

Introduction

1.1 General Introduction

In-process tool failure poses a serious threat to unmanned manufacturing systems, such as flexible machining centers. Developing effective means to monitor and manage cutting tools, in order to avoid off-quality products and/or system damage, presents a significant problem to manufacturing research. Effective tool management requires machinability models that should be as simple as possible yet information regarding tool wear and damage should be obtainable easily. Direct experimentation is typically the basis for tool life and cutting force model.

Drilling is a widely used machining process. It represents approximately 40% of all metal cutting operations performed in industry. Typically, twist drills are used with in a diameter range from 1 to 20 mm. Drill wear and breakage have a direct influence on the dynamic characteristics of the drilling process. A worn drill generates vibration causing the drill to "wander" from its true center or resulting in tapered or oversized hole. These defects are of particular importance in high-speed precision drilling. The machinability models in drilling mainly deal with the following phenomena:

- Tool life of drills,
- Thrust force on the drill,

- Torque on the drill and,
- Surface roughness of the drilled hole.

Several sensing techniques have been used for edge chipping, fracture, wear and poor hole quality. These techniques include touch sensors, power, acoustic emission, torque and/or thrust force and vision system. Thrust force and torque signals are more sensitive to changes in the drill conditions. Hence it is useful to consider drill vibrations in the monitoring of thrust force and torque.

1.2 Vibration in metal cutting

An important practical problem in machining is vibration or "chatter". Chatter has three main adverse effects: it may produce inaccuracies on the work surfaces, it may increase the rate of wear of the tool; and finally it may cause a high-frequency sound which at best is unpleasant and can be physically harmful to near by personnel.

An obvious point to note is that the vibration will involve relative movement of the tool and the workpiece. The work piece can move in almost any direction relative to the tool. Thus under vibrating conditions there may be fluctuations in:

1. The cutting speed (i.e., Surface speed of the tool relative to the work)
2. The feed
3. The inclination of the tool faces with respect to the workpiece surface (i.e., fluctuations in rake angles, clearance angles and cutting-edge angles are possible).

From a knowledge of the cutting process under steady-state conditions it is clear that any of these fluctuations in the cutting process may give rise to fluctuations in the forces on the tool tip. Depending on how these fluctuations are directed and phased relative to the vibration motion, they may either damp or excite the vibration. If

the cutting force fluctuations are large and are opposing the damping effect they may cause the vibration amplitude to grow.

Taylor in his monumental work on the cutting of metals noted the problems which tool vibration may introduce. He suggested that the vibration was due to force variations created by periodic shearing action on chip formation. Kuznestov [1] presents the view that built-up-edge formation can constitute the periodic effect to excite a vibration, irrespective of the natural frequencies of the system. Arnold [2] presented the first systematic study of metal cutting vibrations. He has experimentally investigated the factors which he considered to be of most importance in vibration, i.e., tool sharpness, cutting speed, feed and tool overhang.

Doi and Kato [3] proposed that the self-excited vibration was established due to phase lag of the cutting force behind the vibration movement. Due to this lag effect some energy is available in each oscillation to maintain the vibration. Tobias and Fiswick [4] proposed that dynamic cutting force is a function of feed velocity as well as chip thickness.

From the above discussion of the behavior of cutting process under dynamic conditions, it is clear that there are a large number of factors which may effect the force on the tool. Some instability phenomena appear to be inherent to cutting mechanics, and may initiate force vibrations. Built-up-edge formation, chip segmentation and discontinuous chip formation, depending on the cutting conditions, fall into this category.

1.3 Literature Review

Although several efforts have been made to monitor thrust force and torque in drilling in the past decades, very little has been done to consider the effect of amplitude of relative vibration between the tool and the workpiece on the thrust force and torque which is also a source of fluctuation apart from cutting speed, feed and diameter of drill.

Armarego and Brown [5] presented empirical methods for determining the thrust force and torque in drilling considering feed per revolution and drill diameter. Watson [6] proposed new definitions to cutting tool geometry and found the deficiencies in definitions of some of angles in the ISO and explained how the cutting velocity varies in magnitude and direction from a maximum that is essentially tangential at the outer radius to a minimum value of the feed velocity that is axial at the center of the drill in drilling operation. He derived relations to the tool side rake, tool cutting edge angle and side clearance angle in terms of the drill basic parameters. He proved that on cutting lip, the greatest change in parameters occurs as a function of radius from the center to a point on the lip. He represented a set of relationships interrelating various parameters independent of the back rake and back clearance angles. The effects of radius and feed on the cutting parameters over the cutting lip and chisel edge have also been presented.

Rubenstein [7] has assumed Watson's [6] oblique cutting model to derive the expressions for the torque and thrust force at the lip, chisel edge and margins. In his work relevant values of the chip thickness ratio, the shear stress acting along the shear plane and the friction angle on the rake face were obtained from orthogonal cutting tests performed at several cutting speeds with a variety of tool rake angles and values of these parameters were used to estimate the thrust force and the torque contributions originating at drill lips, chisel edge and margins. But computation of the torque and the thrust force components based on orthogonal models were proved to be very complex. They proposed more tractable, empirical expressions for the torque and thrust force as functions of drill geometry and cutting parameters. These expressions described the dependence of the torque and the thrust on feed, point angle and pre-drilled hole diameter both in absence and in the presence of chisel edge-workpiece contact.

Lin and Ting [8] conducted a series of experiments to study the effects of tool

wear as well as other cutting parameters on the cutting force signals and establish the relation between the force signals and the tool wear as well as other cutting parameters when drilling copper alloy. They conducted experiments by taking four variables: spindle rotational speed ranging from 600 to 2400 rev/min, feed rate ranging from 60 to 200 mm/min, drill diameter ranging from 5 to 10 mm, and average flank wear ranging from 0.1 to 0.9 mm. A statistical analysis provided good correlation between the thrust force and the wear. They also conducted verification experiments to verify the feasibility of the proposed method. Initially they conducted a study to understand the effects of cutting parameters on the cutting force signals. This is because not all cutting parameters have significant effects on cutting force signals, and only parameters with significant effects on cutting force signals have been included in the model of cutting force signals. They selected linear and logarithmic model forms from previously published models. They proposed that the linear model form has better tool wear monitoring capability than the logarithmic model form. The error between the measured and the estimated tool wear was shown to be 0.2 mm.

Lorenz [9] proposed a relatively short, improved method for drill performance testing. Diagonal test plan has been recommended for cutting within a wide range of speeds and feeds. The purpose of multi-level experiments was to assess the curvature of the drill life response surface in experiments of short duration. It was assumed that in the logarithmic system the drill life response surface is represented by the linear and quadratic terms of cutting speed and feed and their interactions. But drill life is mainly a function of drill wear under practical conditions. He has also shown graphically the relation between feed, cutting speed and drill life. The total number of holes drilled is considered as a drill life. He concluded that statistically designed experiments would assist in obtaining more relevant information.

Rubenstein [10] conducted experiments with a set of geometrically similar twist drills to confirm the previously derived expressions relating the torque and the thrust

force to feed and drill diameter in drilling operations. He proposed a model based on assumption that each twist drill is sufficiently large in relation to the chisel edge length for the removal process to be quasi-orthogonal, expressions which have been found to give an accurate representation of the dependence of the torque and thrust force on drill diameter and feed in spade drilling and may be applied to twist drills. He explained the influence of the helix angle on the torque and thrust force generated in twist drilling and its influence on the average rake angle at the lip and hence on the average shear plane angle. The behavior observed with small diameter drills is shown to be consistent with the removal process becoming noticeably oblique. He discussed the consequences of geometrical dissimilarity of drill shape. His model is capable of explaining both the general as well as the exceptional behavior.

Connolly and rubenstein [11] proposed an idealization of the lower boundary of the primary deformation zone in orthogonal cutting on the basis of the experimentally observable processes occurring during chip formation. This boundary is made up of a length L extending from the tool tip in the direction of cutting and a length extending from the extremity of L (remote from the tool tip) at an angle of 45° until it interacts with the free surface of the workpiece(see Fig. 1.1). Using this model and making some simple assumptions regarding stresses acting on this boundary, relation between the cutting force components and geometry of cutting process is simplified. He proved that there is a good correlation between experimental data and these relations. The length L is proposed as an inverse measure of ductility of cutting process. L is shown to be linearly related to adhesion length, i.e., the length of that part of the tool-chip contact region over which the chip adheres to rake face.

Arssecularatne [12] developed a comprehensive review of techniques used to determine tool-chip interface stress distributions. A number of techniques (photo elastic method, split tool method and experimental slip line field method) have been used to determine the distribution of normal and shear stress on the tool rake face during

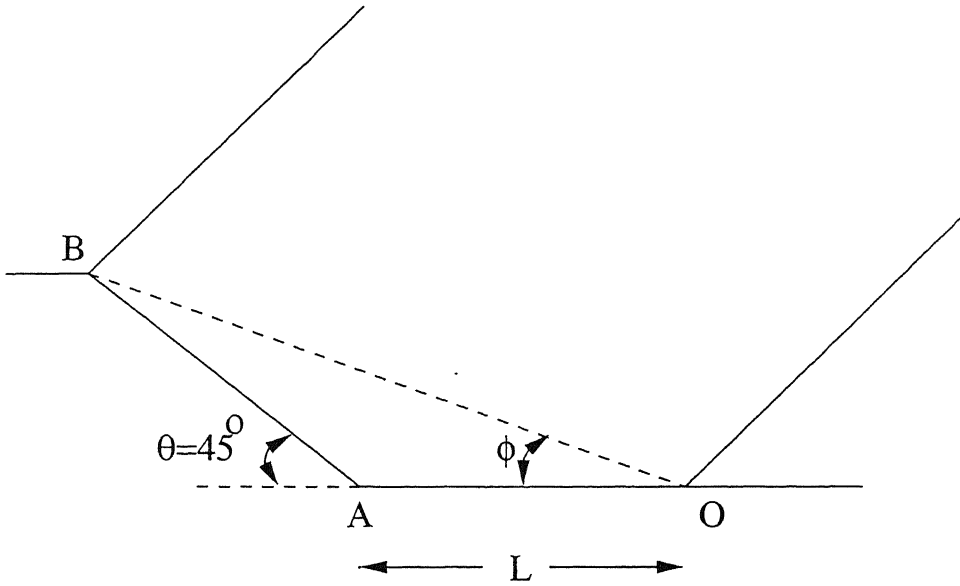


Figure 1.1: An idealized contour of primary deformation zone [11]

machining. The results obtained from split tool tests indicate uniform distributions of shear and normal stresses as the cutting edge is approached which is consistent with the results obtained from slip line field analyses of the chip formation process. He also proposed the methods used to determine the ploughing force in the drilling.

Wardany, Gao and Elbestawi [13] presented a study on monitoring tool wear and tool failure in drilling using vibration signature analysis techniques. Discriminant features, which are sensitive to drill wear and breakage, were developed in both the transverse and the thrust directions, was also investigated. A significant feature, namely the instantaneous ratio of the absolute mean value ($RAMV_i$) was developed in this study and used as a threshold for controlled capture of the vibration signal. The ability of the monitoring features to detect drill wear and breakage was verified experimentally. The drilling tests were performed using 3 and 6 mm diameter high speed steel twist drills and cast iron workpieces.

Subramanian [14] divided the contact zone between tool and work into three main regions; namely, (1) the rake face of the tool (2) the non zero radius of the cutting

edge and (3) the flank " wear land " which rubs against the work surface. He took into account the forces acting on these three regions and derived the expressions for torque and thrust force. Jalaji and Kolarik [15] developed four models from an extensive machinability experiment. Predictive models were developed for tool life, thrust and torque on the drill, and surface roughness of the holes drilled. The research consisted of a laboratory experiment involving four variables; cutting speed, feed, drill diameter and hardness. The effects of machining variables other than speed and feed (i.e, vibration, deflection, and thermal expansion) were ignored in the study. The tool variables such as point angle, relief angles and helix angle were nearly constant.

In the present work effort has been made to study the influence of cutting speed, feed, drill diameter and amplitude of relative vibration between the tool and the workpiece thrust force and torque in drilling. Firstly a theoretical analysis has been presented to study the forces in drilling and then effect of vibration on these force signals. From this thrust force and torque are represented by the linear and quadratic terms of cutting speed, feed, diameter of drill and amplitude of relative vibration between the tool and the workpiece. Experiments have been conducted using planning of experiments. A program has been used to find the co-efficients of empirical relation and the experimental and empirical results were then compared.

1.4 Organization of Thesis

The thesis has been organized in various chapters as follows,

- **Chapter 1** presents the information about the vibrations in cutting and it effects. It also deals with the literature review carried out for the present work.
- **Chapter 2** discusses the theoretical model presented to find thrust and torque in terms of cutting parameters and effect of vibration on force signals.

- In**Chapter 3** experimental setup and procedure are discussed. Planning of experiments and multiple regression analysis have also been elaborated.
- In**Chapter 4** the results obtained from experiments are presented. The effect of various parameters on the thrust force and torque has also been given in this chapter.
- In**Chapter 5** conclusions of the thesis work have been drawn and scope of future work has been elaborated.

Chapter 2

Theoretical Analysis

2.1 Characteristics of Vibration in Drilling

Machining vibrations may be considered in four main categories:

- **Free vibration:** A free vibration of the system following some impact or shock condition. This vibration will decay under the damping action of the machine.
- **A forced vibration from a source other than cutting:** This may be initiated by unbalance in the machine tool drive or by some external dynamic load. In this case the vibration is normally not at a resonant frequency of the machine tool workpiece system.
- **A forced vibration initiated in the cutting process:** The cutting process may have an inherent periodicity which can lead to a forced vibration. An obvious example is that of discontinuous chip formation. In this case also the vibration is usually not at a resonant frequency.
- **Self induced vibration:** A phenomenon in which the vibrational movement causes the cutting process to initiate and maintain the vibration. It may be regarded as negative damping.

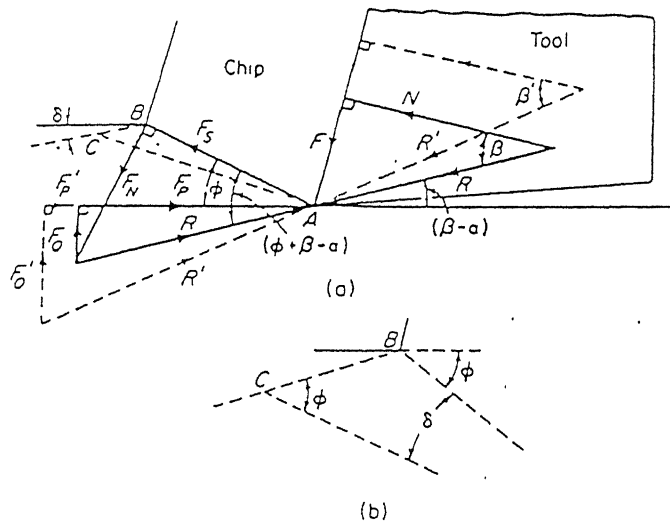


Figure 2.1: Change in Cutting force for an Undeformed chip thickness decreasing due to vibration [16]

Due to production variations, a drill is typically slightly asymmetric. Accordingly, the two corners of the drill point wear gradually, while maximum wear alternates from one cutting edge to the other. This altering process is also considered to be a source of vibration in drilling.

Several authors have reviewed the physical phenomena which may influence force-displacement phase relationships in cutting. Shaw and Holken [16] explain a force lag in terms of fluctuations in the direction of chip approach relative to the tool. Consider the undeformed chip thickness to be decreasing due to vibration of the tool relative to the workpiece, as shown in Fig. 2.1(a).

The rake angle and the cutting velocity can be imagined to change to new values:

$$\alpha_e = \alpha + \delta \quad (2.1)$$

$$N_e = N \cos \delta \quad (2.2)$$

A new shear angle will be formed as

$$\phi_e = \phi + \Delta\phi \quad (2.3)$$

Shaw and Holken [16] assume that the resultant force will be approximately constant in magnitude. This is justified from the fact that the resultant force is approximately constant for small changes in the rake angle under steady-state cutting conditions. Thus, to a first approximation, the new shear plane to be inclined at the angle ϕ to the new direction of the free work surface (see Fig. 2.1(b)). Thus, $\Delta\phi = \delta$, and the new value of friction angle

$$\beta' = \beta + \delta \quad (2.4)$$

The length of the new shear plane will be (see Fig. 2.1)

$$AC = AB + AB\delta \tan^{-1} \phi \quad (2.5)$$

The shear stress τ may be considered constant for small changes δ , Hence the new resultant force is

$$R' = \frac{(AC)b\tau}{\cos(\phi + \beta - \alpha)} = \frac{\tau b(AB)(1 + \delta \tan^{-1} \phi)}{\cos(\phi + \beta - \alpha)} \quad (2.6)$$

The force in the direction of cut becomes,

$$F'_P = R' \cos(\beta - \alpha + \delta) = R(1 + \delta \tan^{-1} \phi) \cos(\beta - \alpha + \delta) \quad (2.7)$$

and Thrust force

$$F'_Q = R' \sin(\beta - \alpha + \delta) = R(1 + \delta \tan^{-1} \phi) \sin(\beta - \alpha + \delta) \quad (2.8)$$

The situation when the undeformed chip thickness increasing due to vibrations shown in Fig. 2.2. From an analysis similar to the above it can be shown that the normal and thrust forces in this case are

$$F''_P = \frac{R \cos(\beta - \alpha + \delta)}{1 + \delta \tan(\phi - \delta)} \quad (2.9)$$

and

$$F''_Q = \frac{R \sin(\beta - \alpha + \delta)}{1 + \delta \tan(\phi - \delta)} \quad (2.10)$$

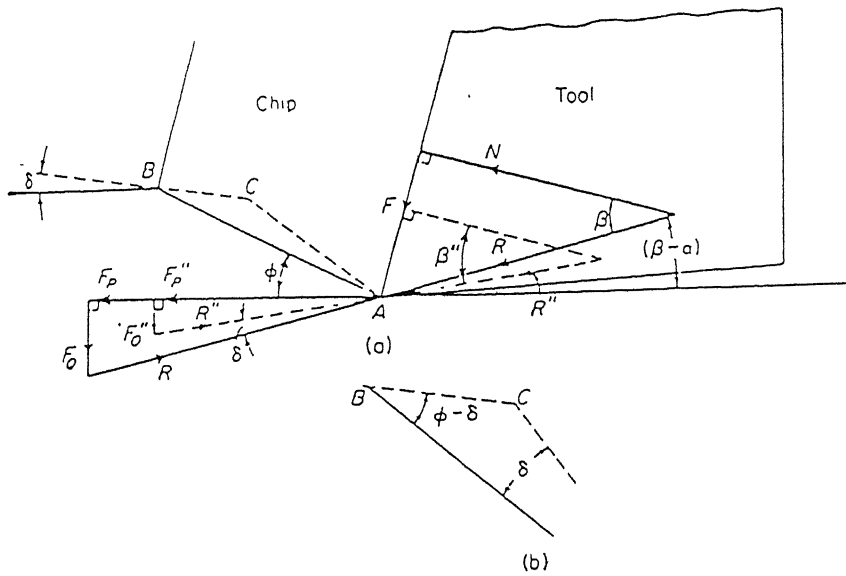


Figure 2.2: Change in Cutting force for an Undeformed chip thickness increasing due to vibration [16]

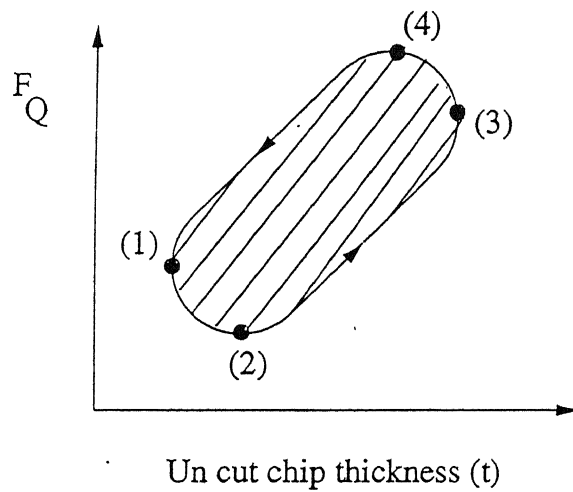


Figure 2.3: Relationship between Thrust force (F_Q) and the undeformed thickness t as the tool vibrates in the path indicated by arrows

Since $[1 + \delta \tan(\phi - \delta)]$ is greater than 1, a comparison of equations (2.7) with (2.9) and (2.8) with (2.10) indicates that the instantaneous forces at any particular depth of cut are higher for decreasing ' t ' (Fig. 2.1) than for increasing ' t ' (Fig. 2.2). This can be represented by a curve as shown in Fig. 2.3. In this figure it can be seen that the minimum and maximum for the force [points (2) and (4), respectively] are reached after the corresponding undeformed chip depth-of-cut minimum and maximum [(1) and (3)]. Thus the change in the undeformed thickness causes the force signals to fluctuate. This model fits the experimental results of Doi and Kato[3].

2.2 Torque and Thrust force in Drilling

It is difficult to conceive of a more complex metal cutting process than one in which the cutting edge of the tool is curved, the rake and clearance faces are not planar and the tool geometry, obliquity and cutting speed vary along the cutting edge, but such is the case of twist drilling. To compound complexity, the lips of the drill are connected by the chisel edge while the outermost ends of the lips terminate at the margins (where the drill rubs against the sides of the hole).

The forces of interest in drilling operations are the thrust force along the axis of rotation and the torque. The side forces acting radially at the cutting edge cancel each other due to the symmetry of the drill. Ghosh and Mallik [17] consider the effect of all the forces acting on the drill (Fig. 2.4) represented by a resisting torque M and a thrust force F . The total thrust force, F can be expressed as

$$F = 2F_T \sin(p) + F_{ch} + F_{friction} \quad (2.11)$$

Where F_{ch} is the force from chisel edge and $F_{friction}$ is the friction force. Similarly, the total moment M can be written as (Fig. 2.4)

$$M = F_C z + M_{ch} + M_{friction} \quad (2.12)$$

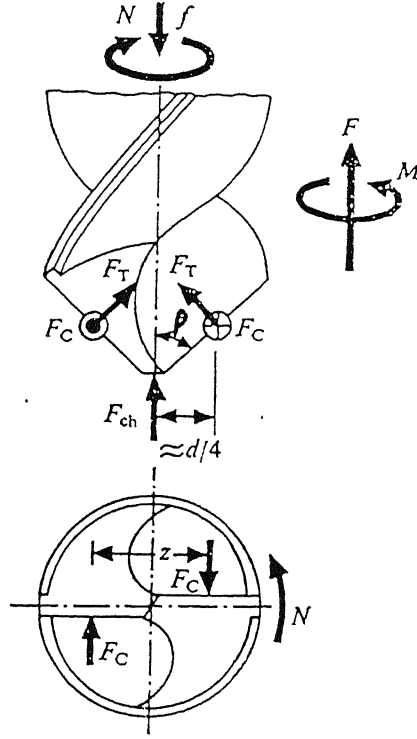


Figure 2.4: Development of Torque and Thrust during drilling

Where M_{ch} is the moment due to chisel edge and $M_{friction}$ is the frictional moment.

Later Rubenstein [7] & [10] presented the concept of the equivalent spade drill in order to demonstrate that expressions for the torque and thrust force generated in spade drilling are applicable to twist drilling. The torque, M and the thrust force, F are each compounded of 3 elements which arise from drill-workpiece contact at the lips, at the web and at the margins, i.e.,

$$M = M_o + M' + M'' \quad (2.13)$$

$$F = F_o + F' + F'' \quad (2.14)$$

Where M_o and F_o originate at the drill lips, M' and F' arise at the chisel edge and

M'' , F'' result from drill-workpiece contact at the margins.

For hole drilling based on theory of orthogonal cutting [11]

$$M_o = \frac{1}{4}(d^2 - c^2) \left[(\mu P_m l / \sin p) + \frac{1}{2} S f (\cot \phi_n + 1) \right] \quad (2.15)$$

$$F_o = \frac{1}{2}(d - c) [2P_m l + P_1 f (\cot \phi_n - 1) \sin p] \quad (2.16)$$

Expressions for M' and F' , appropriate to removal at the chisel edge, can be derived from the above equations and are given by [7]

$$M' = \frac{1}{4}c^2 \left[\mu_c P_m l_c + \frac{1}{2} S f (\cot(\phi_n)_c + 1) \right] \quad (2.17)$$

$$F' = \frac{1}{2}c [2P_m l_c + (P_1)_c f (\cot(\phi_n)_c - 1)] \quad (2.18)$$

The origin of the torque, M'' and the thrust, F'' generated at the margins was not investigated in depth so far; however, in a very limited investigation it was show that both M'' and F'' are linear functions of the feed. Although the influence of drill diameter was not examined, it seems reasonable to infer that M'' will be proportional to ' d ' so that it can be written

$$M'' = k_1 d + k_1 d f \quad (2.19)$$

$$F'' = K_2 + k_2 f \quad (2.20)$$

Substitution from equations (2.15) to (2.20) into equations (2.13) and (2.14), as appropriate, results in the following expressions: [see **Appendix A**]

$$M = (k_1 + k_1 f) d + [(E + G m^2) + (B + H m^2) f] d^2 \quad (2.21)$$

$$F = (k_2 + k_2 f) + [(J + Q m) + (U + V m) f] d \quad (2.22)$$

So the torque and the thrust force in drilling depends on the feed and the diameter of the drill. But experimental investigation made by Lin and Ting [8] revealed that these factors depend on the cutting speed also. The change in undeformed thickness which

is due to vibrations causes variations in force signals in cutting. Therefore in the present work the amplitude of relative vibration between the tool and the workpiece has been considered as a measure of vibration.

Finally from above discussion it can be concluded that the thrust force and the torque in twist drilling can be expressed as a function of the cutting speed, feed, diameter of the drill and amplitude of relative vibration between the tool and the workpiece. .

Chapter 3

Experimental Procedure and Set-up

3.1 Vibration measuring system

A vibration measuring system used in the present work consists of the following components:

- Accelerometer
- Pre-amplifier
- Amplifier

3.1.1 Accelerometer:

The accelerometer is an electromechanical transducer. The transducing element consists of two piezoelectrical (Lead Zirconium Titanate) discs on which is resting a heavy mass (see Fig. 3.1). The mass is pre loaded by a stiff spring and the whole assembly is mounted in a metal housing with a thin base. When the accelerometer is subjected to vibration, the mass will exert a variable force on the piezoelectric discs. This force is exactly proportional to the acceleration of the mass. Due to the piezoelectric effect a variable potential will be developed across the two discs, which is proportional to

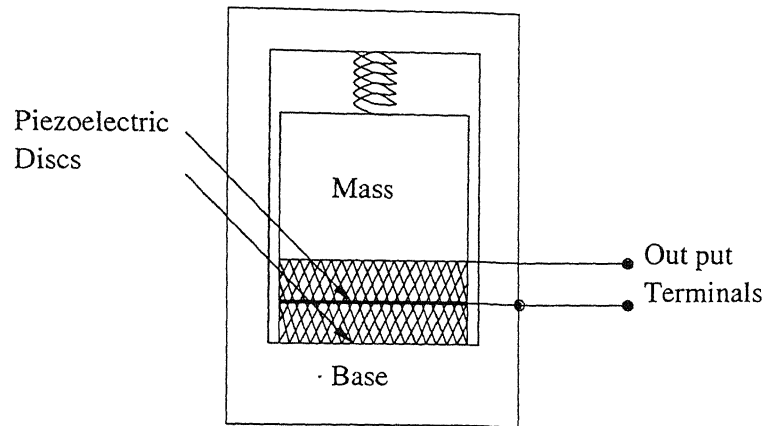


Figure 3.1: Schematic drawing of a piezoelectric accelerometer

the force and therefore to the acceleration of the mass. This potential has been picked up from the output terminals of the accelerometer and used for determination of the vibration amplitude.

A proper mounting of the accelerometer to the specimen is of utmost importance when measurements are taken. The accelerometer has been mounted with a permanent magnet which gives electrical isolation from the vibrating specimen. A closed magnetic path has been used and there is virtually no magnetic field at the accelerometer position.

3.1.2 Pre-amplifier:

Pre-amplifiers are used for conversion of the rather weak transducer signal into a stronger signal which can be handled by the succeeding storage or read-out equipment. The vibration pick-up amplifier is designed for use in vibration measuring systems and constitutes an important link between the accelerometer and the appropriate measuring amplifier. The pre-amplifier mainly consists of two-stage amplifier, a set of integrating networks and a built-in shaker table for calibration purposes. By selecting various built-in integrating networks, the acceleration dependent signal derived from the accelerometer has been converted into a signal which is proportional to the velocity

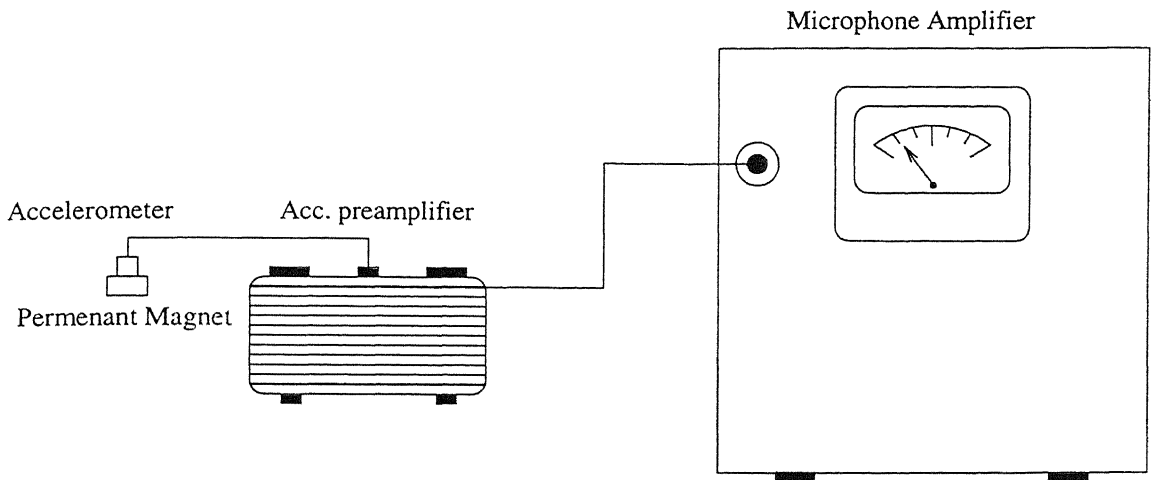


Figure 3.2: Set-up for vibration measurement on the workpiece

or displacement of the object under investigation.

3.1.3 Microphone Amplifier:

The Microphone Amplifier is a very versatile measuring instrument which, when used in conjunction with suitable transducers, can be employed in a great variety of fields. It is primarily designed for acoustical, electro-acoustical and vibration measurements. Basically it consists of two independent amplifier sections which may either be connected in cascade or have a filter system interposed between them. The power supply contains the necessary rectifiers and filters for the operation of the amplifiers and supplies the power to external condenser microphone or pre-amplifier in use.

3.1.4 Displacement Measurement

The accelerometer has been mounted with a permanent magnet on the workpiece. The output voltage from the accelerometer is fed to the CONDENSER MICROPHONE input socket of the Microphone Amplifier via a pre-amplifier (see Fig. 3.2) The INPUT SWITCH of the Microphone Amplifier has been set to position "Condenser Microphone" and the FREQUENCY RESPONSE SWITCH to position "Linear 2 - 40000"

and it has been checked that the indicating meter does not show a higher voltage. If necessary, the voltage can be brought below the stated peak voltages by attenuating the input voltage to the pre-amplifier with control knob "Attenuation". RMS type of detection has been selected by the "Meter switch" on indicating apparatus. The integration switch on the pre-amplifier has been set to position "Displacement". The displacement in cm derived as follows:

The read value in volts \times the value (10 , 10^{-1} or 10^{-3} cm) indicated by integration switch \times the value indicated by the switch "Attenuation" of the pre-amplifier.

3.2 Measurement of forces in Drilling

The measurement of the thrust force required to overcome the resistances in the direction of feed and the torque required to rotate the drill are essentially involve in drilling, reaming, tapping, counter boring, and such similar processes. There is a choice of measuring the forces at the drill-spindle end or at the table workpiece end. The latter approach is more popular in view of simple and stationary devices involved.

The available literature [18] reviews the following types of dynamometers for the drilling and allied purpose like reaming, tapping, counter boring etc.

- Measuring the forces at the drill end
 1. Dynamometer based on recurrent pulse technique
 2. Dynamometer for the fine tapping by Sokelovskii
 3. Torquemeter by Dean And Kilburn
- Measuring the forces at workpiece end/ table end
 1. Tube element dynamometer
 2. Spoked wheel dynamometer

3. Two component dynamometer

Out of above choices spoked wheel dynamometer is selected in the present work because any eccentricity present between the drill and the dynamometer axes never affects the accuracy of the results.

3.2.1 Principle of dynamometer

The working principle of the dynamometer used is shown in Fig.3.3. This consists of a spoked wheel (usually four spokes) having a stiff inner hub and an outer rim. By rigidly clamping either the inner hub or the outer rim to the machine table and applying the drilling torque and thrust to the unclamped rim of hub, it is possible to deform the spokes in cantilever configuration in the planes of the torque and thrust as shown in Fig. 3.4. The strains due to the application of thrust force and torque has been measured by applying strain gauges on the points of maximum strain. The strain gauges mounted near the fixed ends of the four cantilevers in full-bridge configuration give the torque and the thrust experienced by the system as shown in Fig. 3.5(a)&(b). The analysis of the spokes indicates that for best results the sections should be identical and identically located with respect to the inner boss and the outer rim both in radial and axial directions. Further the fillet radius at the junction of the spoke elements to the ring portions should be the same for all the spokes. This type of dynamometer is characterized by higher sensitivity for both torque and thrust force, low rigidity and lower natural frequency, but it also has fabricational difficulty, as it is preferable to machine the entire wheel and spokes from one piece.

3.2.2 Working of dynamometer in the present case

In the present case the dynamometer was required to measure the thrust force, F and torque, M . For measuring thrust force, F , strain gauges were cemented on the top and the bottom portions of the spokes (1 to 8) which were connected to form the

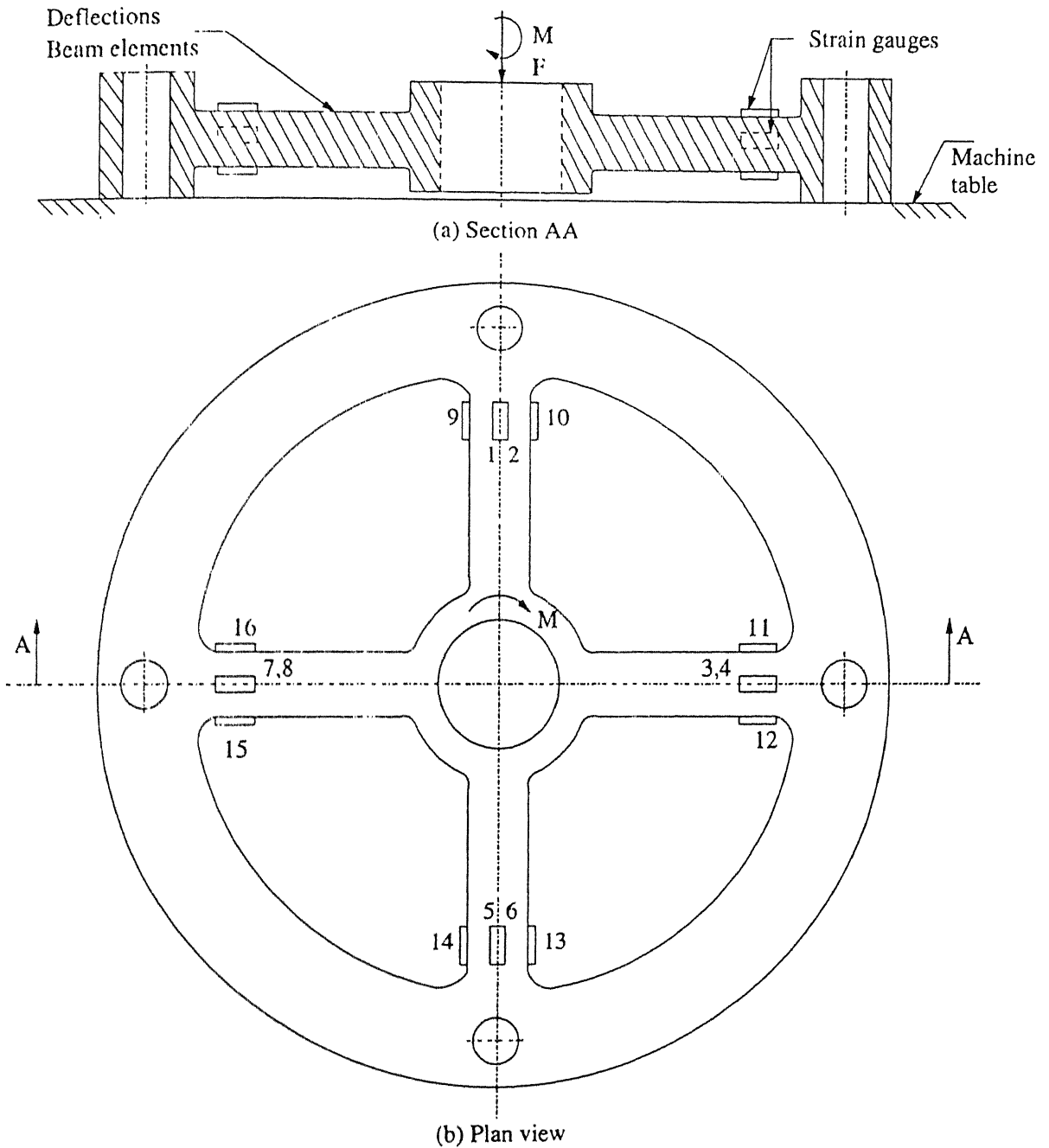
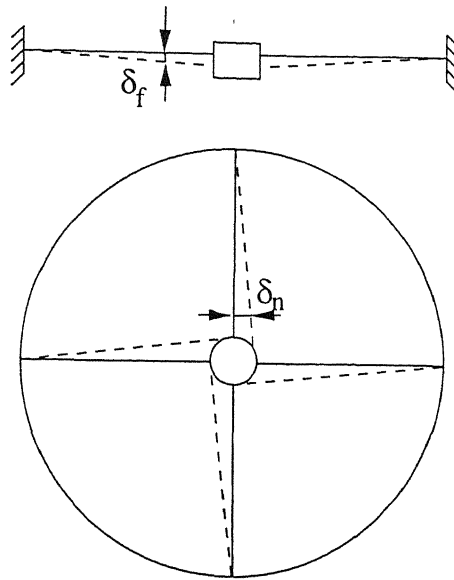


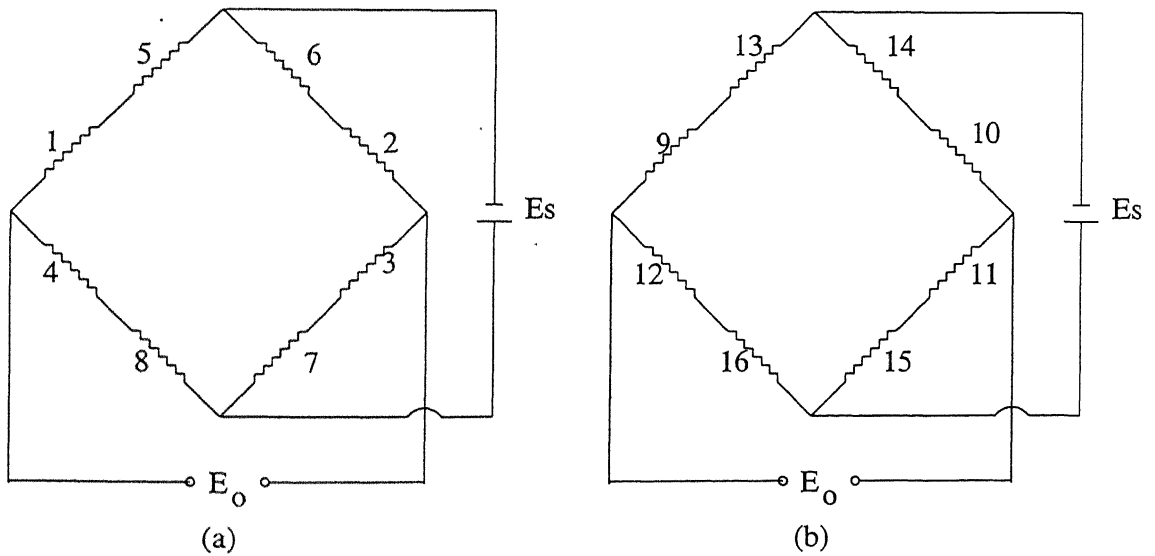
Figure 3.3: Spoked-wheel dynamometer for the measurement of drilling thrust(F) and torque(M).



δ_f = Deflection due to Thrust F

δ_n = Deflection due to Torque M

Figure 3.4: Deflection scheme of spoked-wheel



E_s = Input Voltage 5 V D.C. E_o = Output Voltage

Numbers 1 to 16 shows strain gauges indicated in Fig.3.3.

Figure 3.5: Wheatstone bridge for measurement of (a) Thrust force (b) Torque.

Wheatstone bridge as shown in Fig. 3.5(a).

A potentiometer was connected across the bridge. The recorder performed the function of a galvanometer here. The resistance of the potentiometer was varied till no current flowed through the recorder i.e., the recording pen came to a standstill position resulting in a balanced Wheatstone bridge. Then the cutting process was started. The thrust force acting on dynamometer deformed the strain gauges 1 to 8 and as a result the bridge was unbalanced due to change in resistance. This change in resistance (i.e., change in force) was reflected through the curves recorded on the paper. The dynamometer was initially calibrated using known static loads. Finally the value of vertical force was quantified by using calibration curve. The procedure above was followed for torque, M in which strain gauges numbered 9 to 16 were deformed. The Wheatstone bridge for the torque is shown in Fig. 3.5(b).

3.3 Multiple Regression Analysis

A regression model that involves more than one regressor (independent) variable is called a multiple regression model. When there are more than one independent variables influencing the response variables, the multiple regression method is adopted to build the model. Before starting to build an empirical model it is essential to understand the range (of variables) in which model has to be developed, since the developed model may be linear in some part of the range and non-linear in some other part. However if the range is very wide, there is less chance for the model to be linear. In real life situations a linear model is very rarely encountered, but at the same time, a second order model is usually good enough to capture a great deal of information [19]. To build a second order model at least a three-level experimental design or plan is needed.

3.3.1 Design for fitting second order model

A design by means of which observed values of the response are collected for estimating the parameters in the second order model (Eq. 3.1) is called a second-order design.

$$y = \beta_o + \sum_{i=1}^k \beta_i x_i + \sum_{i=1}^k \beta_{ii} x_i^2 + \sum_{i=1}^{k-1} \sum_{j \neq i}^k \beta_{ij} x_i x_j + \epsilon \quad (3.1)$$

Where x_1, x_2, \dots, x_k are the input variables which influence the response, y . $\beta_o, \beta_i (i = 1, 2, \dots, k), \beta_{ij} (i = 1, 2, \dots, k, j = 1, 2, \dots, k.)$ are constants, and ϵ is a random error (contribution of factors not considered in Eq.3.1). Since model (3.1) contains pure quadratic terms, second-order experimental design must involve at least three levels of each input variables.

3.3.2 Least square estimation of the regression coefficients

The method of least squares is typically used to estimate the regression coefficients in a multiple linear regression model. Least square estimate minimizes the sum of squares of the deviation between the model and the data. The method tries to minimize the sum of squares of the residual. A model with $n > k$ observations ($k = \text{no: of independent variables } x_i \text{ and } n = \text{no: of experiments}$). y_i denoting the i th observed response and x_{ij} denoting the i th observation or level of regressor x is as shown below.

$$y = \beta_o + \beta_1 x_{i1} + \beta_2 x_{i2} + \dots + \beta_k x_{ik} + \epsilon_i \quad (3.2)$$

Here ϵ_i is the random error. Assumptions made about errors are:

1. random errors have zero mean and common variance.
2. random errors are mutually independent in the statistical sense.
3. random errors are normally distributed.

The method of least squares chooses the $\beta_0, \beta_1, \dots, \beta_k$ in the equation 3.2 so that the sum of the errors ϵ_i is minimized. The above equation can be expressed in the matrix notation as

$$y = X\beta + \epsilon \quad (3.3)$$

where

$$y = \begin{bmatrix} y_1 \\ y_2 \\ \vdots \\ y_n \end{bmatrix} \quad X = \begin{bmatrix} 1 & x_{11} & x_{12} & \dots & x_{1k} \\ 1 & x_{21} & x_{22} & \dots & x_{2k} \\ \vdots & \vdots & \vdots & & \vdots \\ 1 & x_{n1} & x_{n2} & \dots & x_{nk} \end{bmatrix}$$

$$\beta = \begin{bmatrix} \beta_1 \\ \beta_2 \\ \vdots \\ \beta_k \end{bmatrix} \quad \text{and} \quad \epsilon = \begin{bmatrix} \epsilon_1 \\ \epsilon_2 \\ \vdots \\ \epsilon_n \end{bmatrix}$$

The sum of squares of the errors has to be minimized because the some of the error terms might be positive and some might be negative. The task is to minimize the deviation from the actual data. The sum of squares of the residual can be written as

$$\sum_{i=1}^n \epsilon_i^2 = (y - X\beta)^T(y - X\beta) \quad (3.4)$$

The least square estimate minimizes the sum of the residuals at the experimental points. Equation (3.4) is differentiated with respect to the β terms and equating all partial derivatives to zero and solving for β terms the least squares estimates for the model is obtained. When the input matrix is denoted in the format given below, then least squares estimator of β is

$$\beta = (X^T X)^{-1}(X^T y) \quad (3.5)$$

where the vector β is the estimate of the parameters and X is the input variable matrix and y is the response variable vector.

The data $[x_i, y_i]$ may be obtained from any of the statistical experimental designs.

3.4 Planning of experiments

If an experiment is to be performed most efficiently, then a scientific approach to planning of experiment must be employed. By the statistical design of experiments, we refer to the process of planning the experiments so that appropriate data could be collected, which may be analysed by statistical methods resulting in valid and objective conclusions.

The difference in true output response and calculated output response must be determined. The order in which data will be collected and the method of their randomization to be employed must be determined prior to the experiment. A mathematical model for the experiment must also be proposed, so that a statistical analysis of data could be performed.

Many experiments involve in a study of effects of two or more input variables on the output response. It can be shown that, in general, factorial designs are most efficient for this type of experiment. By a factorial design, it is meant that in each complete trial or replication of the experiment, all possible combinations of the levels of the input variables are investigated. The effect of an input is defined as the change in output response produced by the change in the level of the input variables.

Factorial designs are generally preferred because they are more efficient than one factor-at-a-time experiments. Furthermore, a factorial design is necessary when interactions may be present, to avoid misleading conclusions. Finally factorial designs allow effects of an input to be estimated at several levels of the other inputs, yielding conclusions that are valid over a range of experimental conditions.

In the present case, three factorial (3^3) design has been adopted i.e., a factorial arrangement of 3 input variables (speed, feed, and diameter of drill) each at 3 levels. Without any loss of generality, the 3 levels of each input can be referred as low (0), intermediate (1), and high (2). Each treatment combination in the 3 factorial design will be denoted by 3 digits as shown in Fig. 3.6, where the first digit indicates the

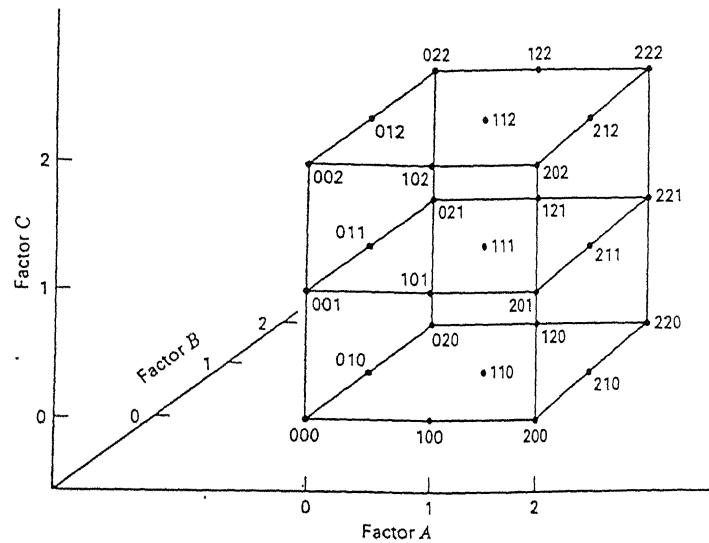


Figure 3.6: Treatment combinations in a 3^3 design

level of speed, the second digit indicates the level of feed, and the third digit indicates the level of drill diameter. For example, 012 indicates that the experiment should be carried out at low level of speed(0), intermediate level of feed (1) and high level of drill diameter(2). Similarly there will be 27 number of experiments.

3.5 Experimental Procedure

For the experiments, C-45 steel was used as the workpiece material and HSS twist drills as cutting tool. The material composition and the tool geometry are given in the **Appendix B** . The tool geometry was maintained uniformly for all the experiments. RM-61 type radial drilling machine was used to conduct the experiments. According to planning of experiments, 3 levels of speed, feed and drill diameter was chosen from machining data hand book and limiting ranges of machine, as:

- Cutting speed : 80, 150, 220 rpm
- Feed : 0.12, 0.2, 0.3 mm/rev

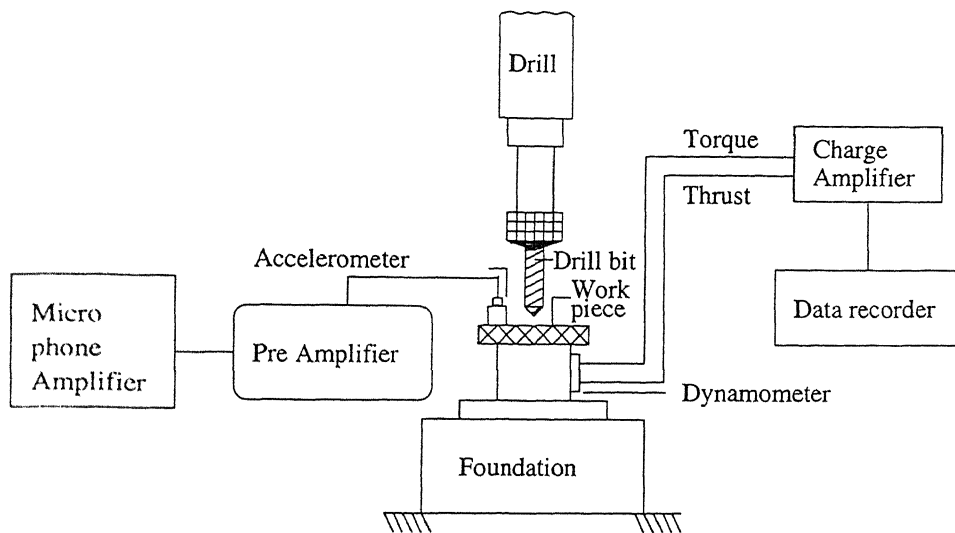


Figure 3.7: Schematic diagram of experimental set-up

- **Dia: of drill** : 14, 16, 18 mm

Schematic diagram of experimental set-up is shown in Fig. 3.7. The spoked-wheel dynamometer was made water proof in order to prevent the possibility of short-circuit. The workpiece was fixed on the dynamometer with the help of a cover plate and screws. The dynamometer was connected to the potentiometer and a recorder. Before actual machining process was started, the dynamometer was calibrated and Wheatstone bridge was balanced by the potentiometer manually. The accelerometer for vibration pickup was placed on the workpiece with some distance away from the center of the drill and this sensor position was maintained for all experiments. The output of the accelerometer was then connected to a Microphone Amplifier through a pre-amplifier. At a particular cutting condition (speed, feed and diameter of drill), the thrust force (F), torque (M) and amplitude of relative vibration between the workpiece and the tool values were recorded. The procedure was repeated for all the 27 sets of experiments. From the recorded forces, average thrust force and torque and from the Microphone Amplifier, R.M.S value of amplitude were found out.

Chapter 4

Results and Discussions

The experiments were conducted to study the influence of the speed, feed, diameter of drill and amplitude of relative vibration between the tool and workpiece on the thrust force and the torque in drilling. The experiments were carried out as discussed in the planning of experiments. To conduct the experiments C-45 steel was used as the workpiece material and standard HSS drills as cutting tool. The material composition and the tool geometry were given in the **Appendix B**. Twenty seven experiments (3^3 factorial design) were used to develop the second order polynomial in the form of a regression equation. The set of input cutting parameters and output response are given in Table 4.1, which have been used to find the constant terms in the equation (3.2).

The models for the thrust force and the torque derived from the data shown in table 4.1 are as follows.

$$\begin{aligned} \text{Thrustforce } F = & -3814 - 2N - 2290f + 711d + 20272A - \\ & 7Nf + 365fd + 25858f^2 - 18d^2 \end{aligned} \quad (4.1)$$

and

$$\begin{aligned} \text{Torque } M = & 9.6068 + 0.0280N - 32.1839f - 1.1364d + \\ & 35.9957A - 0.0228fN - 0.0022Nd + 2.0343fd + \\ & 13.7537f^2 + 0.0388d^2 \end{aligned} \quad (4.2)$$

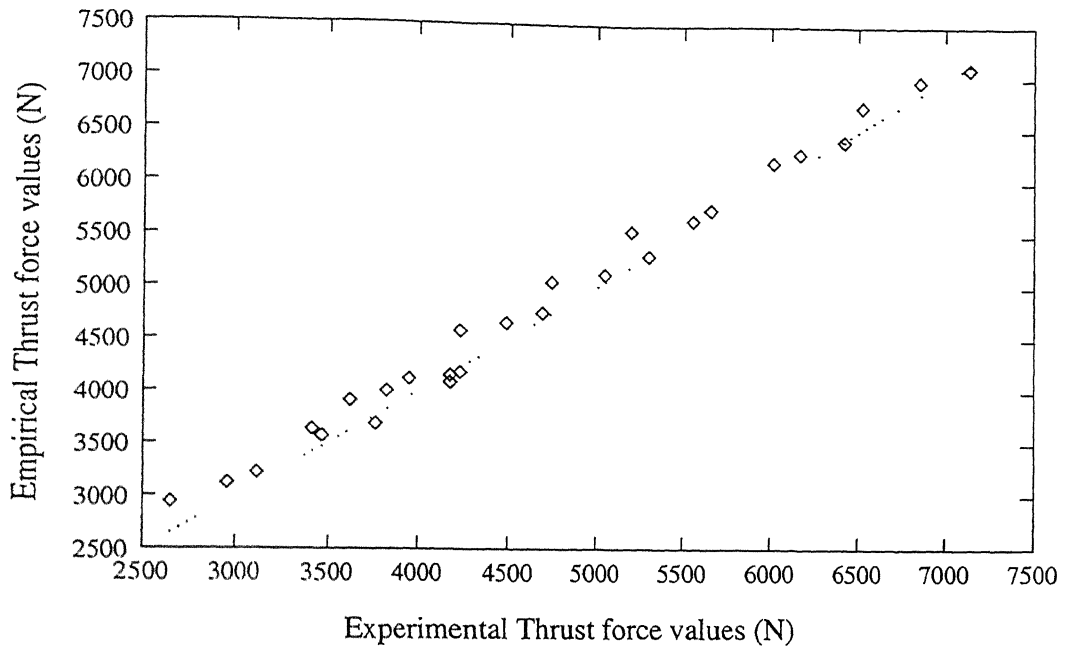


Figure 4.1: Comparison of Experimental and Empirical Thrust force values

Where N = Cutting Speed (rpm), f = Feed (mm/rev), d = Diameter of Drill (mm), A = Amplitude of relative vibration between the tool and the workpiece (mm), F = Thrust force (N), and M = Torque (N-m).

From the model it can be seen that the amplitude of relative vibration between the tool and workpiece influence the thrust force and torque as well as cutting speed, feed, diameter of drill. So by knowing amplitude of relative vibration between the tool and workpiece and cutting conditions we can easily monitor the force signals in drilling.

4.1 Validation of Regression Model

The second order polynomial regression model is developed for thrust force and torque. Fig 4.1 and 4.2 show the comparison of the thrust force and torque signals measured from the experiments and those estimated from the regression models respectively (Eq 4.1 and 4.2). In the above diagrams all the points nearly fall on a 45° line which

Experiment Number	Speed (rpm)	feed (mm/rev)	Diameter of Drill(mm)	Amplitude of Vibration(mm)	Experimental Values	
					Thrust Force(N)	Torque (N-m)
1	80	0.12	14	0.006	3118.81	0.7928
2	80	0.2	14	0.012	4229.76	0.9373
3	80	0.3	14	0.014	5656.67	1.3522
4	80	0.12	16	0.008	3760.92	1.3445
5	80	0.2	16	0.016	4688.41	1.6672
6	80	0.3	16	0.019	6421.08	2.0168
7	80	0.12	18	0.017	4178.80	1.7449
8	80	0.2	18	0.026	5299.94	2.8683
9	80	0.3	18	0.033	7134.54	4.1830
10	150	0.12	14	0.011	2955.74	0.6761
11	150	0.2	14	0.019	4178.80	0.8605
12	150	0.3	14	0.023	5554.75	1.1371
13	150	0.12	16	0.012	3465.35	0.9681
14	150	0.2	16	0.023	4484.57	1.1294
15	150	0.3	16	0.027	6166.28	1.4521
16	150	0.12	18	0.025	3949.48	1.1951
17	150	0.2	18	0.029	5045.14	2.2230
18	150	0.3	18	0.041	6854.25	3.1313
19	220	0.12	14	0.012	2649.97	0.6146
20	220	0.2	14	0.022	3618.23	0.7068
21	220	0.3	14	0.032	5198.02	0.9527
22	220	0.12	16	0.025	3414.38	0.8605
23	220	0.2	16	0.031	4229.76	1.0756
24	220	0.3	16	0.037	6013.40	1.2370
25	220	0.12	18	0.029	3822.07	0.7888
26	220	0.2	18	0.037	4739.37	1.0039
27	220	0.3	18	0.043	6523.01	2.3903

Table 4.1: Experimental Data

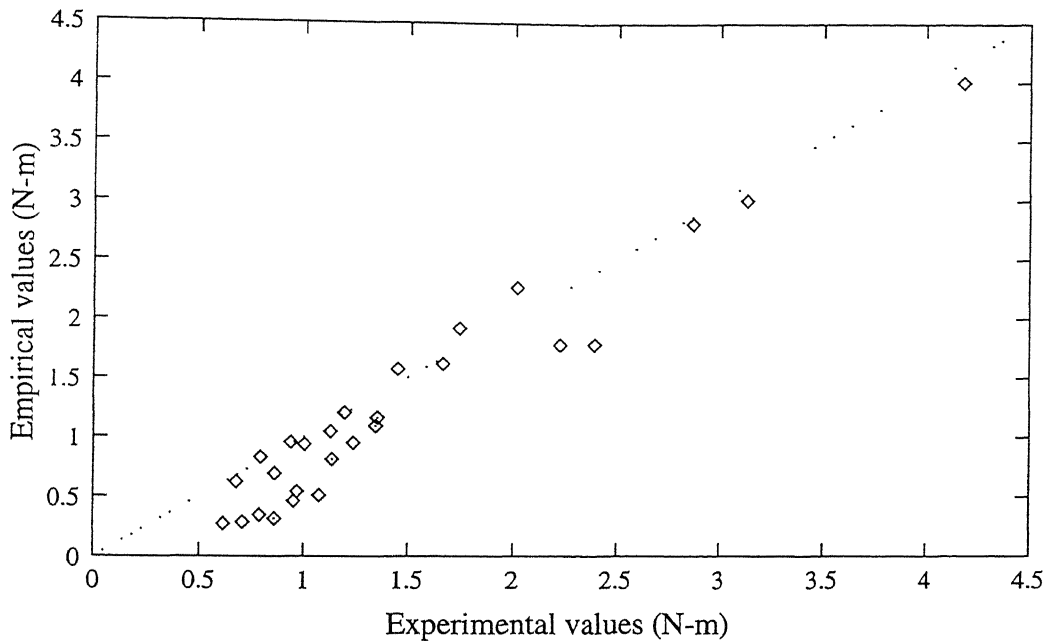


Figure 4.2: Comparison of Experimental and Empirical Torque values

is the ideal case. The correlation co-efficient between experimental values and the predicted values has been found out be 0.979541 in case of thrust force and 0.888792 in case of torque respectively. Thus it can be stated that our developed regression models predicts the values of the thrust force and torque reliably over the selected range of input cutting parameters.

4.2 Feasibility Study

In the previous section, force signal models have been established. Good correlation between the force signals measured and those estimated from the force signal models is shown. The force signal models can be used to estimate the thrust force and torque by knowing the amplitude of vibration between the tool and the workpiece and other cutting parameters. Additional tests are conducted to examine the feasibility of these models to estimate thrust force and torque. Table 4.2 shows the cutting parameters and experimental values for the additional tests. Fig 4.3 & 4.4 show the comparison

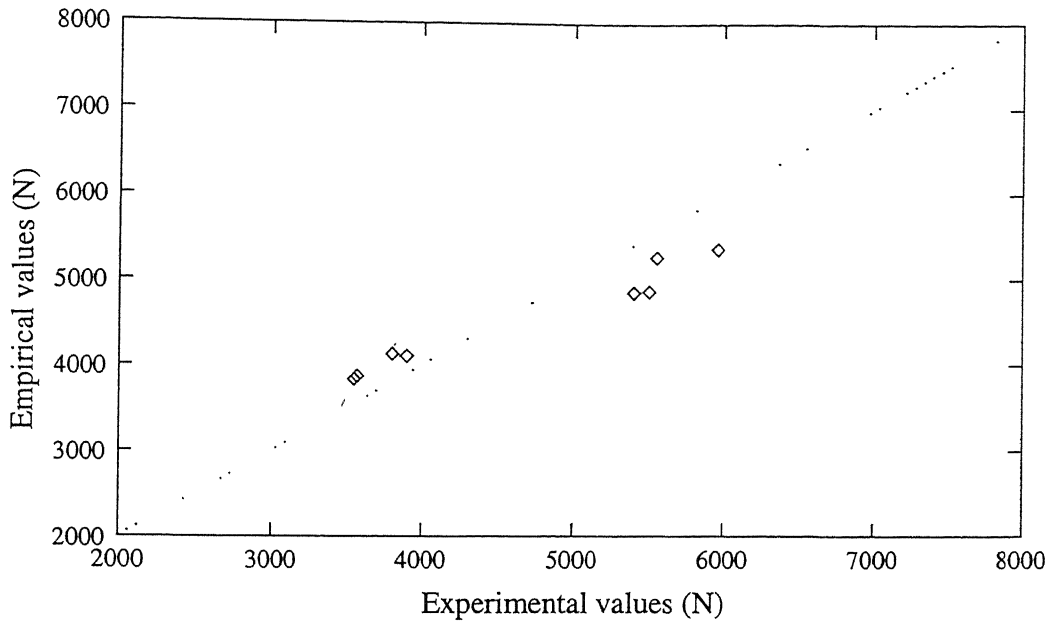


Figure 4.3: Comparison between Experimental and Empirical Thrust force values for additional verification tests

of thrust force and torque signals measured from the experiments and those estimated from the above models for additional tests. In which case also it can be seen that all points nearly fall on 45° line which is ideal case.

4.3 Effect of various parameters

For studying the effect of given input parameters on the thrust force and torque, the regression equation is reduced with only two parameters viz., the output parameter thrust force and one of the input parameters, the effect of which on the output parameter has to be established. This is done by assigning an optimum constant value to all other input parameters at which the thrust force as well as the torque is minimum. The optimum value for a particular parameter is selected from the Table 4.1 within its working range. After getting the reduced equation, the values of thrust force and torque over a range of values of input parameter were calculated. Plots are drawn between these values of force signals and the values of parameters individually,

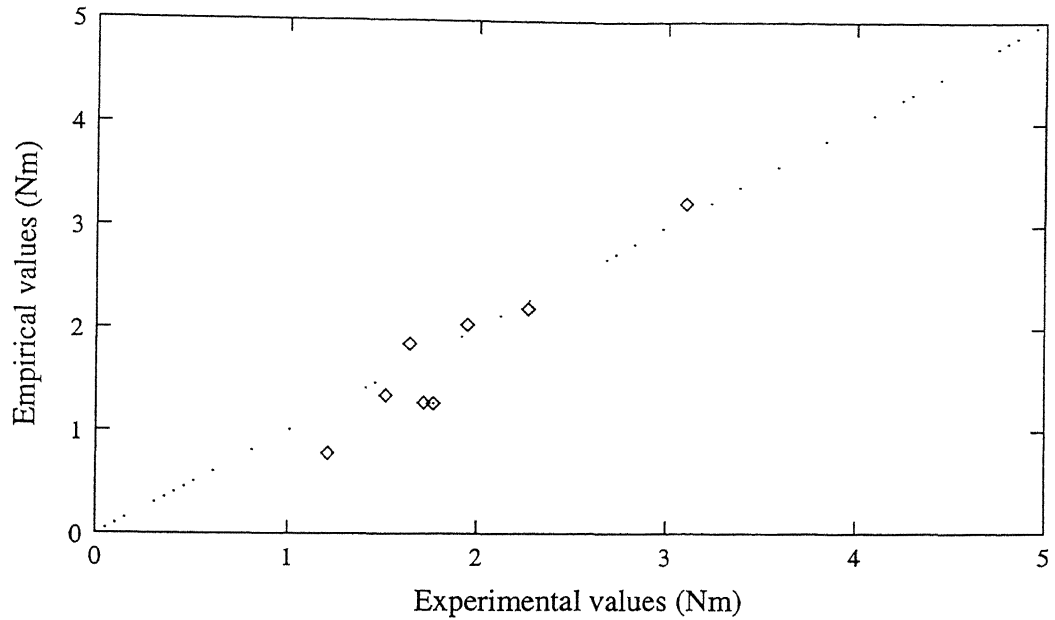


Figure 4.4: Comparison between Experimental and Empirical torque values for additional verification tests

Experiment Number	Speed (rpm)	feed (mm/rev)	Diameter of Drill(mm)	Amplitude of Vibration(mm)	Experimental Values	
					Thrust Force(N)	Torque (N-m)
1	80	0.12	17	0.009	3567.26	1.5185
2	80	0.2	17	0.012	5503.78	1.6451
3	80	0.12	19	0.010	3898.15	1.9474
4	80	0.2	19	0.023	5962.43	3.1023
5	150	0.12	17	0.017	3546.88	1.2148
6	150	0.2	17	0.023	5401.86	1.7716
7	150	0.12	19	0.021	3801.68	1.7210
8	150	0.2	19	0.030	5554.74	2.2645

Table 4.2: Cutting conditions and Experimental results for additional verification tests

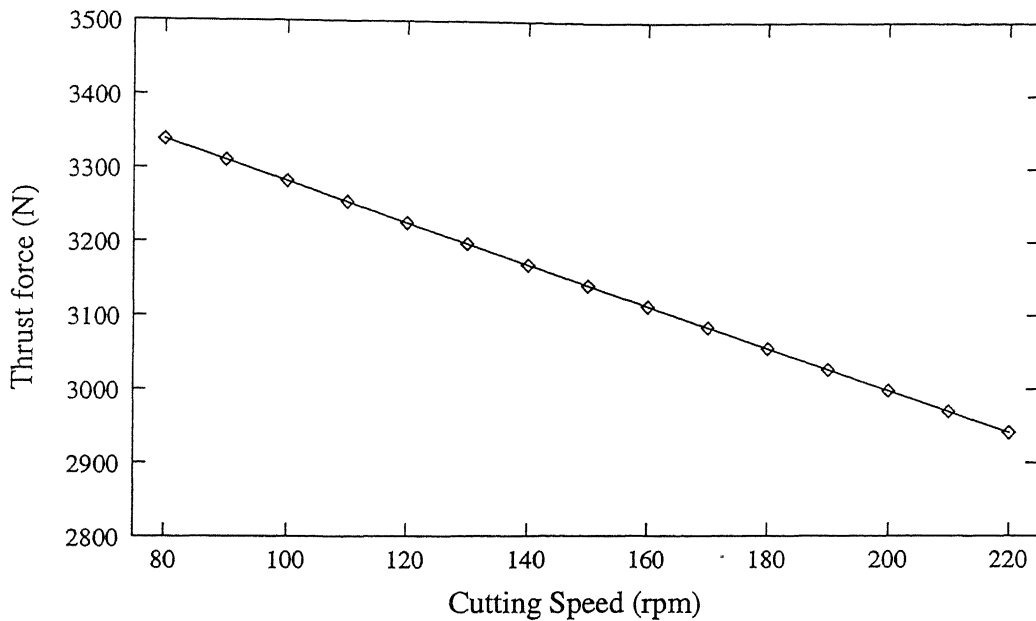


Figure 4.5: Cutting speed vs Thrust force

with the corresponding parameter on the X-axis and force signals on the Y-axis. The various plots obtained are shown in the following figures.

Fig 4.5 & 4.6 show the effect of spindle rotational speed on the thrust force and torque respectively. It is found that cutting force signals are both decreased linearly as the spindle rotational speed increases. This is so since the product of cutting speed and cutting force determines the power which is consumed at the cutting edge it is evident that the utilization of the power of a given machine tool requires a reduction in cutting force if cutting speed increases. Another possible reason is the following: Theoretically, the cutting temperature will increase as cutting speed increases [20]. One might expect that the strength of work material may decrease as temperature increase which is large enough to cross the recrystallization temperature where strain hardening is not very effective. In other words, the cutting force may decrease as cutting speed increases owing to the decrease of work material strength.

Fig 4.7 & 4.8 show the effect of amplitude of vibration on cutting force signals. It is shown that both the thrust force and torque increase as amplitude of vibration

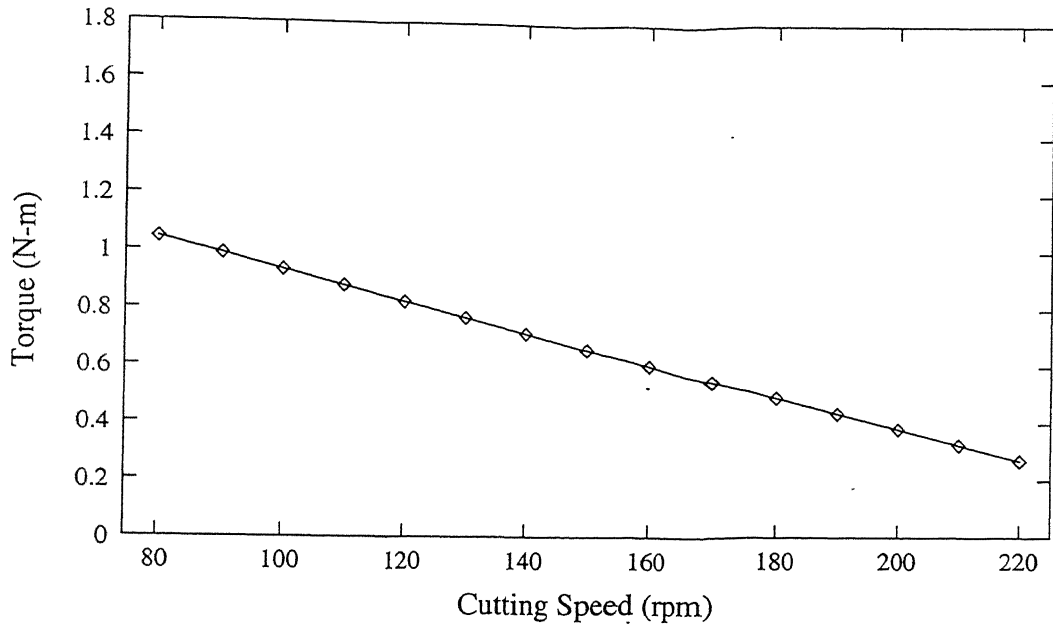


Figure 4.6: Cutting speed vs Torque

increases. This is due to the increase of friction between the tool and the work piece.

It is generally known that the cutting force will increase as chip load increases. Fig 4.9 & 4.10 shows the main effect of feed on the thrust force and the torque respectively. The results indicate that the thrust and torque vary similarly with feed under all cutting conditions. The increase in the torque and thrust with feed can be explained by the increase in chip thickness during cutting at higher feeds which requires greater cutting force to overcome the greater resistance to plastic deformation.

Fig 4.11 & 4.12 show the effect of drill diameter on cutting force signals. It is found that the cutting force signals both increase as the drill diameter increases. the thrust force and torque increase is proportional to the square of drill diameter as given in Eq:4.1 & 4.2.

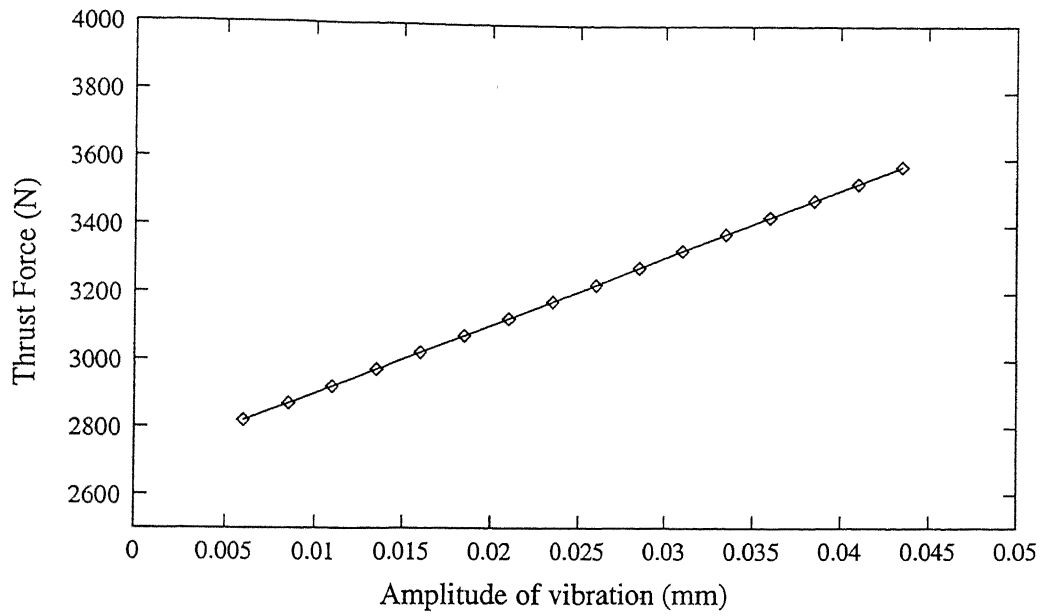


Figure 4.7: Amplitude of vibration vs Thrust force

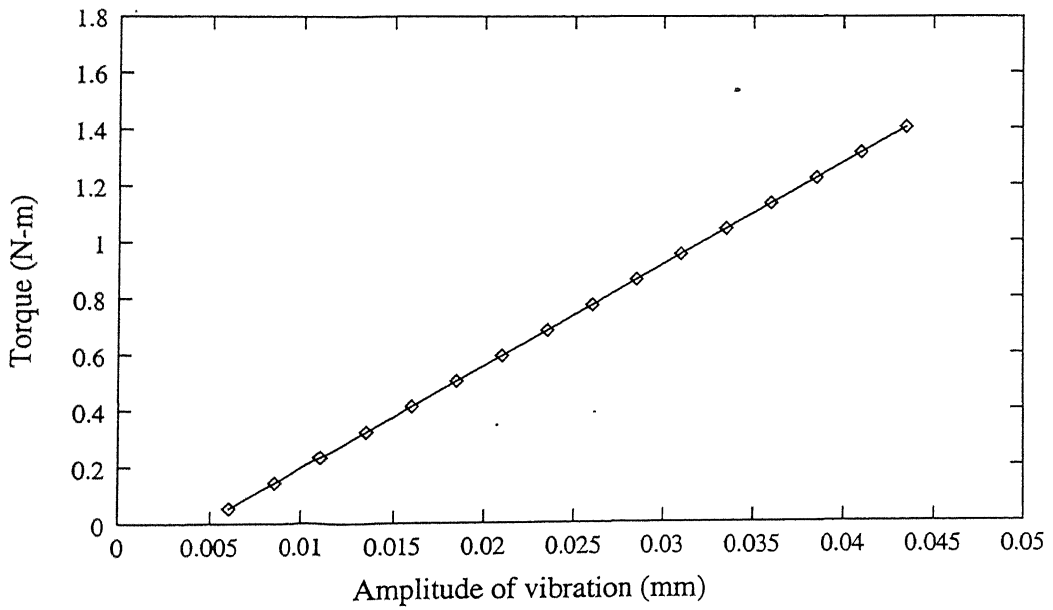


Figure 4.8: Amplitude of vibration vs Torque

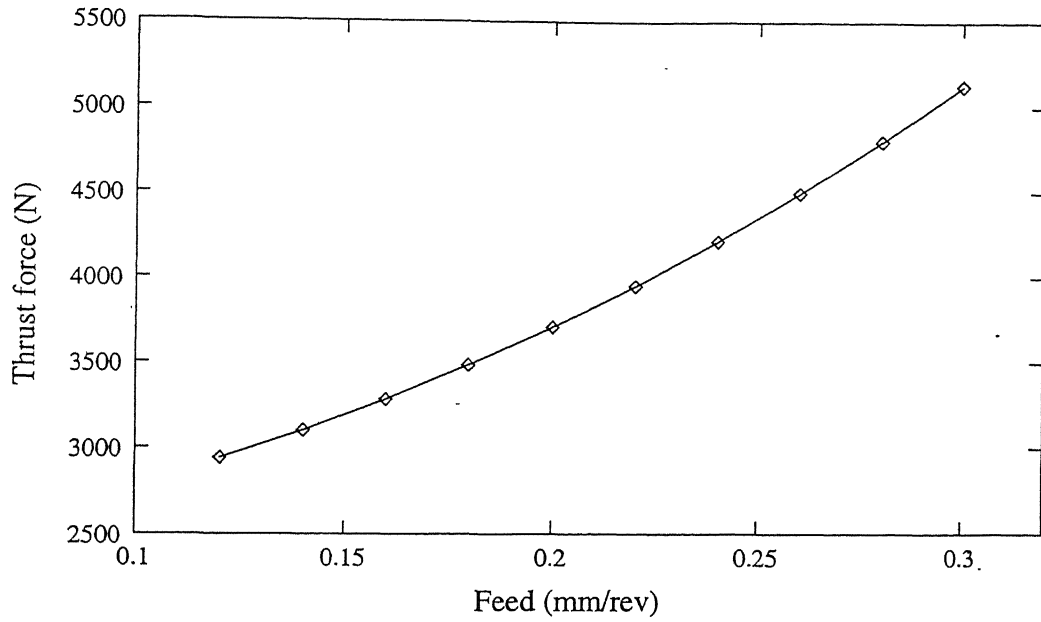


Figure 4.9: Feed vs Thrust force

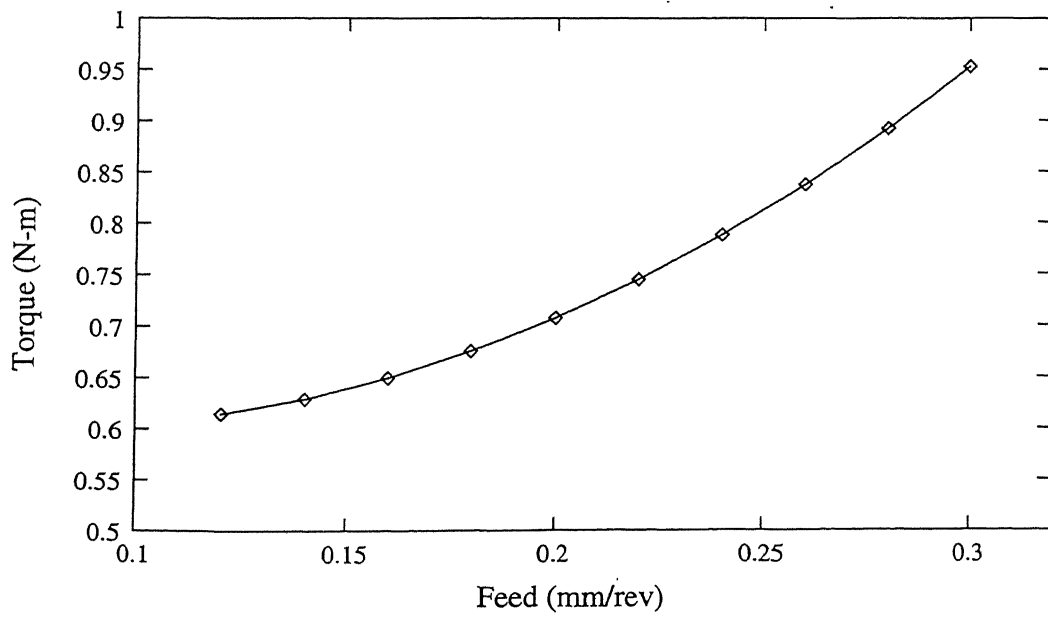


Figure 4.10: Feed vs Torque

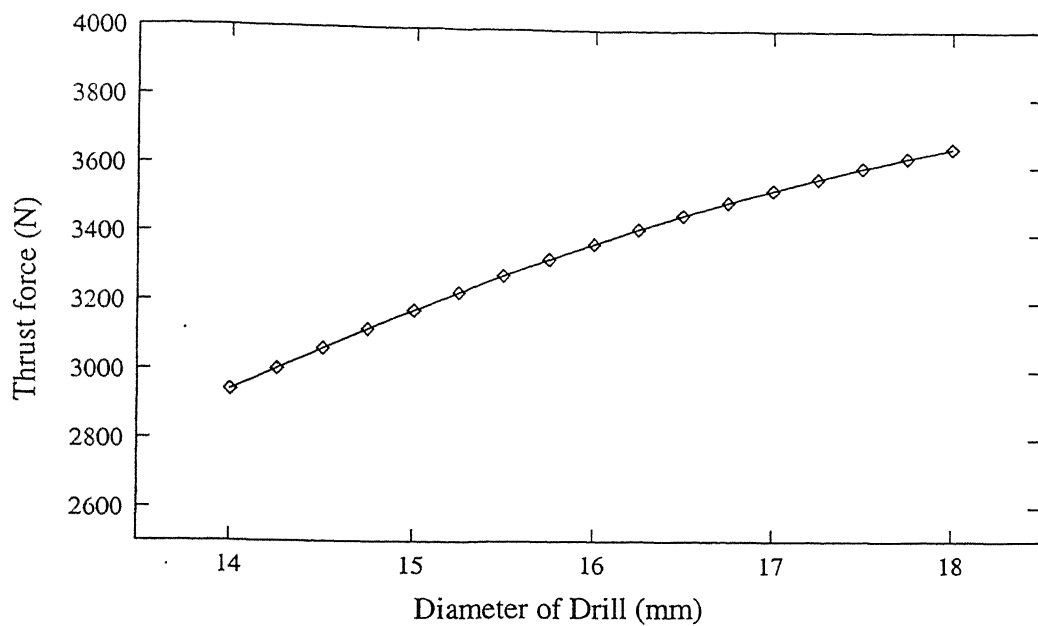


Figure 4.11: Diameter of Drill vs Thrust force

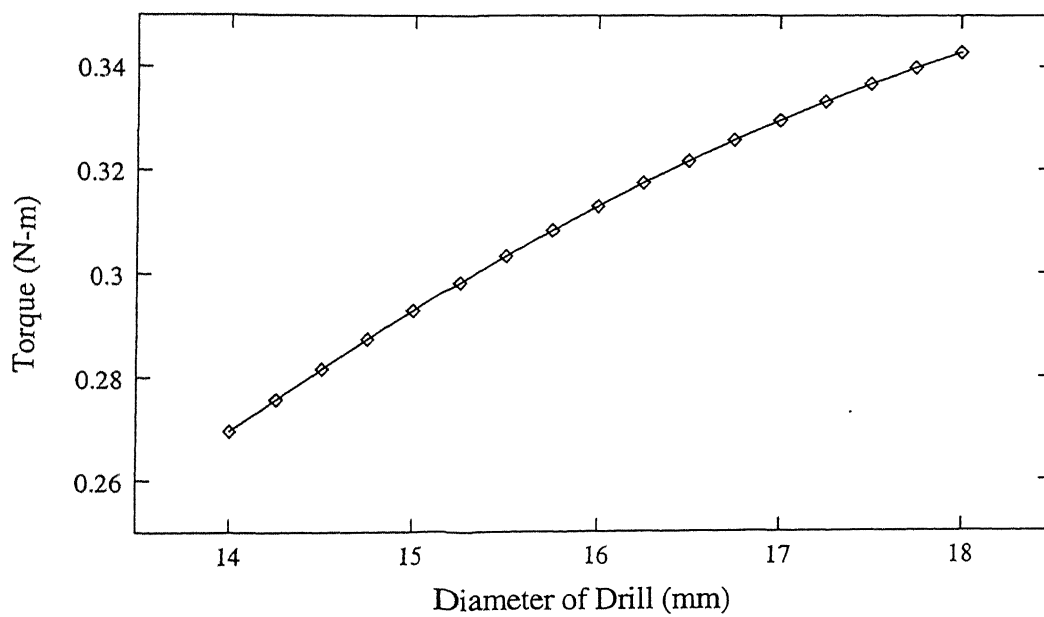


Figure 4.12: Diameter of Drill vs Torque

Chapter 5

Conclusions and Scope of future work

5.1 Conclusions

In this work the basic aim of force monitoring in drilling has been fulfilled. A second order regression model has been developed through which force monitoring can be made which can be used in design of machine tools, jigs and fixtures, to select economic cutting conditions as well as a tool failure criterion.

The following objectives have been achieved:

1. For force monitoring in drilling, a second order regression model has been developed.
2. For collection of the experimental data to develop regression model, a special design like the 3^3 factorial design is used successfully.
3. Comparison is done between the experimental values and the predicted values and the correlation coefficient found out be 0.979541 for the thrust force and 0.888792 for the torque which shows that the models can be used for force monitoring.

4. The effect of various factors on the force signals has been studied independently using the polynomials of regression equation.

5.2 Scope of the future work

The following areas have been identified for the future work:

1. Other parameters which will effect the force signals can be explored to be included in the model such as deflection of the tool, Thermal expansion and hardness of workpiece material.
2. The regression model for force monitoring consisting vibration can be developed for other conventional processes like turning, shaping and milling.
3. The present developed mathematical model can also be checked for large number of experimental data in order to minimize the experimental error further by the implementation of a different design of experimentation.

References

- [1] Kuznetsov, V.D., "Metal transfer and built up - in friction and cutting", (E.H.Freitag. ed.) Oxford : Pergamon Press Ltd., 1966.
- [2] Arnold, R.N., "The mechanism of tool vibration in the cutting of steel", Proc. Inst. Mech. Enggrs., Vol. 154, 1946, pp 261.
- [3] Doi, S., and Kato, S., "Chatter vibrations of lathe tools", Trans. Amer. Soc. Mech. Enggrs., Vol. 78, 1956, pp 1127.
- [4] Tobias, S.A., and Fishwick, W., "The chatter of lathe tools under orthogonal cutting conditions", Trans. Amer. Soc. Mech. Enggrs., Vol. 80, 1958, pp 1079.
- [5] Armarego, E.J.A., and Brown, R.H., "The machining of metals", Prentice-Hall, Inc, New jersy, 1969.
- [6] Watson, A.R., "Geometry of Drill Elements", Int. J. Mach. Tool. Des. Res., Vol. 25, No. 3, 1985, pp 209-227.
- [7] Rubenstein, C., "The torque and thrust force in twist drilling-I. Theory", Int. J. Mach. Tools Manufact, Vol. 31, No. 4, 1991, pp 481-489.
- [8] Lin, S.C., and Ting, C.J., "Tool wear monitoring in drilling using force signals", Wear, Vol. 180, No. 1, 1995, pp 53-60.
- [9] Lorenz. G., "A contribution to the standardization of drill performance tests", Annals of CIRP, Vol. 25, No. 1, 1977, pp 39-43.

- [10] Rubenstein, C., "The torque and thrust force in twist drilling-II. Comparison of experimental observations with deductions from theory", *Int. J. Mach. Tools Manufact.*, Vol. 31, No. 4, 1991, pp 491-504.
- [11] Connolly, R., and Rubenstein, C., "The mechanics of continuous chip formation in orthogonal cutting", *Int. J. Mach. Tool Des. Res.*, Vol. 8, No. 3, 1968, pp 159-187.
- [12] Arsecularatne, J.A., "On tool-chip interface stress distributions, Ploughing force and size effect in machining", *Int. J. Mach. tools Manufact.*, Vol. 37, No. 7, 1997, pp 885-899.
- [13] El-Wardany, T.I., Gao, D., and Elbestaw, M.A., "Tool condition monitoring in drilling using vibration signature analysis", *Int. J. Mach. Tools Manufact.*, Vol. 36, No. 6, 1996, pp 687-711.
- [14] Subramanian, K., and Cook, N.H., "Sensing of drill wear and prediction of tool life", *J. Engg. Ind. Trans ASME*, Vol. 99, 1977, pp 295-301.
- [15] Jalali, S.A., and Kolarik, W.J., "Tool life and machinability model for drilling steels", *Int. J. Mach. Tools Manufact.*, Vol. 31, No. 3, 1991, pp 273-282.
- [16] Shaw, M.C., and Holken, W., "On self excited vibrations in metal cutting", *Industrie anzeiger*, Vol. 6, No. 63, August, 1957, pp 35.
- [17] Ghosh, A., and Mallik, A.K., "Manufacturing Science", East-West Press Private limited, New Delhi, 1985.
- [18] Venkatesh, V.C., and Chandrasekaran, H., "Experimental techniques in metal cutting", Prentice-Hall of India Private Limited, New Delhi, 1987.
- [19] Montgomery, D.C., "Design and analysis of experiments", 4 th edition, John wiley & sons, New York, 1997.

- [20] Shaw, M.C., "Metal cutting principles", Oxford University Press, Oxford, 1984.

Appendix A

Forces in Drilling

$$M = M_o + M' + M'' \quad (\text{A.1})$$

and

$$F = F_o + F' + F'' \quad (\text{A.2})$$

For hole drilling based on orthogonal cutting

$$M_o = \frac{1}{4}(d^2 - c^2) \left[(\mu P_m l / \sin p) + \frac{1}{2} S f (\cot \phi_n + 1) \right] \quad (\text{A.3})$$

$$F_o = \frac{1}{2}(d - c) [2P_m l + P_1 f (\cot \phi_n - 1) \sin p] \quad (\text{A.4})$$

$$M' = \frac{1}{4}c^2 \left[\mu_c P_m l_c + \frac{1}{2} S f (\cot(\phi_n)_c + 1) \right] \quad (\text{A.5})$$

$$F' = \frac{1}{2}c [2P_m l_c + (P_1)_c f (\cot(\phi_n)_c - 1)] \quad (\text{A.6})$$

$$M'' = k_1 d + k_1 d f \quad (\text{A.7})$$

$$F'' = k_2 + k_2 f \quad (\text{A.8})$$

Substituting $A = \frac{1}{4}\mu P_m l$; $B = \frac{1}{2}S(\cot \phi_n + 1)$; $C = \frac{1}{4}\mu_c P_m l_c$;

$D = \frac{1}{8}S(\cot(\phi_n)_c + 1)$ into equations (A.3) and (A.5) we have

$$\begin{aligned} M_o &= (d^2 - c^2) [(A / \sin p) + B f] \\ &= d^2(1 - m^2) [(A / \sin p) + B f] \end{aligned} \quad (\text{A.9})$$

$$M' = c^2(C + Df) = m^2 d^2(C + Df) \quad (\text{A.10})$$

Substituting equations (A.9), (A.10) and (A.5) into equation (A.1) gives

$$\begin{aligned} M &= \left[\left[(A/\sin p)(1 - m^2) + Cm^2 \right] + \left[B(1 - m^2) + Dm^2 \right] f \right] d^2 + k_1 + k_1 df \\ &= (k_1 + k_1 f)d + \left[(E + Gm^2) + (B + Hm^2)f \right] d^2 \end{aligned} \quad (\text{A.11})$$

Where $E = A/\sin p$; $G = C - E$; $H = D - B$.

Similarly, substituting $J = P_m l$; $L = \frac{1}{2}P_1(\cot \phi_n - 1)$; $N = P_m l_c$; $P = \frac{1}{2}(P_1)_c(\cot(\phi_n)_c - 1)$ in equations (A.4) and (A.6)

$$F_o = (d - c)(J + Lf \sin p) = d(1 - m)(J + Lf \sin p) \quad (\text{A.12})$$

$$F' = c(N + Pf) = md(N + Pf) \quad (\text{A.13})$$

Substituting equations (A.12), (A.13) and (A.8) into equation (A.2) gives

$$\begin{aligned} F &= (k_2 + k_2 f) + \left[[J(1 - m) + Nm] + [L(1 - m) \sin p + Pm] f \right] d \\ &= (k_2 + k_2 f) [(J + Qm) + (U + Vm)f] d \end{aligned} \quad (\text{A.14})$$

Where $Q = N - J$; $U = L \sin p$; $V = P - U$.

Appendix B

Specifications

Work material	: C-45 (Medium carbon steel).
Workpiece specifications	: 0.40-0.50%C; : 0.05-0.35%Si; : 0.6-0.9%Mn; : 0.055%S(max); : 0.05%P(max).
Cutting tool material	: H.S.S.
Cutting tool composition	: 18%W, 4%Cr, 1%V.
Drill specification	: Diameters 14, 15, 16,17,18, 19 mm; : Point angle 118° ; : Lip clearance angle 13° ; : Chisel edge angle 128° ; : Helix angle 30° .

Specifications of Drilling machine : Type RM 61;

- : Max drilling radius 1190mm;
- : Min drilling radius 530mm;
- : Diameter of column sleeve 350mm;
- : Max drill head traverse 660mm;
- : Available number of feeds 6 (0.12-1.25);
- : Available number of speeds 12 (40-1700);
- : Overall height of machine 2710mm;
- : 3 speed sliding gear box.

Accelerometer : Type 4312 BRUEL & KJAER;

- : Sensitivity 45-65 mv/g;
- : Frequency range 2-6000 Hz;
- : Height 22mm;
- : Material Base - Steel.

Pre-amplifier : Frequency range 2-20000Hz;

- : Max: Output Voltage 20V;
- : Power supply 100-240 V, 50 or 60 Hz;
- : Minimum measuring level 20μ .

Amplifier : Type 2603 A BRUEL & KJAER;

- : Frequency Characteristic "Linear" 2-40000Hz;
- : Power supply 100-240 V A.C, 50-400Hz.



129554

Date Slip

129554

This book is to be returned on the
date last stamped.

[illegible]